BUTTERWORTH HEINEMANN

Polymer Vol. 36 No. 16, pp. 3143–3150, 1995

0032-3861/95/$10.00 + 0.00

Influence of hydrogen bonding on the viscoelastic properties of thermoreversible networks: analysis of the local complex dynamics

M. Müller
Max-Planck-Institut für Polymerforschung, Ackermannweg 10, 55128 Mainz, Germany

and U. Seidel and R. Stadler*
Institut für Organische Chemie, Becherweg 18–22, Johannes-Gutenberg-Universität Mainz, 55099 Mainz, Germany
(Received 14 November 1994)

The viscoelastic properties of thermoreversible polybutadiene networks in which junctions are formed by binary contacts between polar stickers (phenylurazole) are investigated by dynamic mechanical spectroscopy within the frequency range 0.0079–79.5 Hz (0.05–500 rad s^{-1}). Time–temperature superposition is applicable in the terminal flow region and the glass transition regime, whereas thermorheologically complex behaviour is observed within the rubbery plateau region. For the terminal relaxation zone the polar stickers enhance the relaxation time and broaden the relaxation time spectrum. The thermorheologically complex behaviour within the rubbery plateau region results from the occurrence of an additional relaxation process which is attributed to the process of complexation/decomplexation of the reversible hydrogen bond contacts. The characteristic relaxation time of this process at 233 K is 0.044 s. This process can also be monitored in dielectric relaxation. Discrepancies between dynamic mechanical and dielectric data are discussed.

(Keywords: thermoreversible network; hydrogen bonds; dynamics)

INTRODUCTION

Polybutadienes which are functionalized statistically by a small number of 4-phenyl-1,2,4-triazolidine-3,5-dione units (phenylurazole (U)) represent a class of model thermoreversible networks[1]. The relaxation behaviour of such a system, in which the polar stickers form binary contacts via hydrogen bonding (*Figure 1*), will be governed by

1. the number of units per chain, i.e. the chain length and the degree of functionalization;
2. the thermodynamics of the complex, i.e. the fraction of complexed urazole units x_{U_2} which is given by the concentration $[U]_0$ and the equilibrium constant $K = f(T)$; and
3. the dynamics of complexation and decomplexation.

Based on the earlier work of Gonzales[2,3], Leibler, Rubinstein and Colby (LRC) developed a theoretical model (the sticky reptation model) based on a renormalization of the reptation model[4]. In this theory, the stress relaxation modulus of a thermoreversible network is described (*Figure 2*). At short times $t < \tau_e$ (where τ_e is the characteristic Rouse relaxation time of an entanglement strand), the behaviour is governed by local relaxations and the transition to the glass. At times $\tau_e < t < \tau$ (where τ is the lifetime of binary contacts), the material will behave like a covalently crosslinked network with a shear modulus

$$G(t) = G_N^0(t) + \nu(t)RT \quad (1)$$

where G_N^0 is the rubbery plateau modulus attributable to the entanglement network without stickers and $\nu(t)RT$ is the modulus contribution from the hydrogen bond links. As soon as the experimental timescale exceeds the lifetime of binary contacts, the temporary junctions will not contribute to the plateau modulus any more. As a consequence, the modulus will drop to the value for the entanglement network. The terminal relaxation which occurs at t_D^0 in the absence of stickers will be shifted to longer times t_D owing to a decreased self-diffusion coefficient[4] for the chains in such a thermoreversible network.

Though polybutadienes with U stickers have been studied intensively by dynamic mechanical spectroscopy[5–8], infra-red spectroscopy[6,9] and, more recently, by optical rheometry[10] and dielectric spectroscopy[11], a number of problems remain unsolved or have not been adequately addressed. In previous work, the experimental set-up limited the dynamic mechanical measurements to the analysis of the terminal zone (with the

* To whom correspondence should be addressed

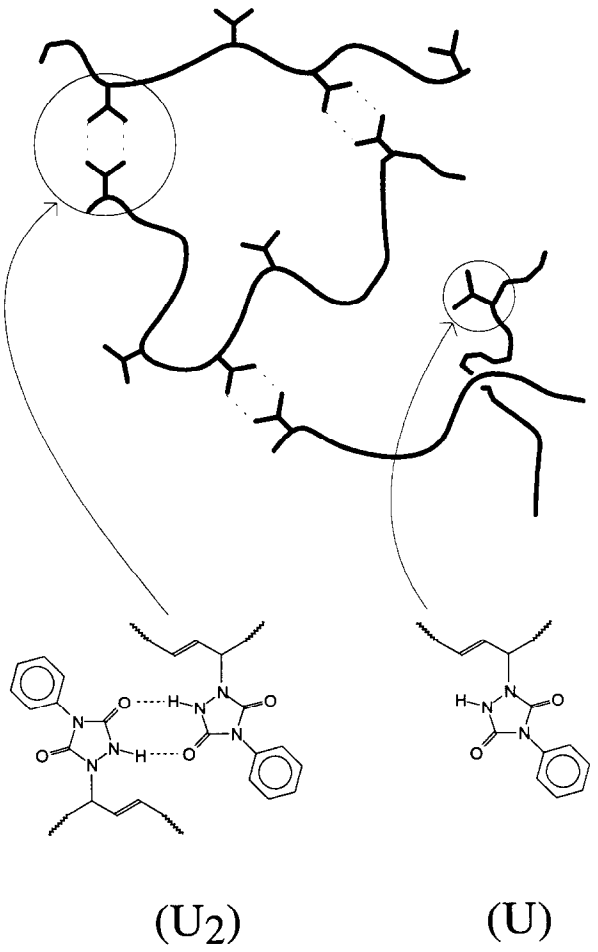

Figure 1 Thermoreversible network with open (U) and binary (U_2) phenylurazole contacts

storage modulus $G' < 5 \times 10^6$ Pa and an experimental frequency range of 0.044–7.5 Hz). The polar stickers lead to a shift in the terminal zone to lower frequencies[5], an increased zero shear viscosity[12] and a considerably broadened relaxation time spectrum[10]. Analysis of the viscoelastic properties over a broad frequency range has been based on the applicability of the time–temperature superposition (TTS) principle. It has been known for some time that TTS should not be strictly applicable because the relaxation of chain segments and the dynamics of the hydrogen bond complexes should follow different temperature dependences. However, in the frequency range accessible, TTS appears to be valid in the terminal relaxation zone. Besides the shift in the terminal relaxation which was described in previous work[5,8], first hints of a 'high frequency relaxation' which was only observed in one sample[5,8] were attributed to the dynamics of complexation/decomplexation (in the following designated as the α^*_{DMA} relaxation), as predicted by the sticky reptation model.

With a newer experimental set-up, it is now possible to analyse the relaxation behaviour of the thermoreversible networks over much wider frequency and temperature ranges using different sample geometries. A preliminary experiment has been performed by Colby and Stadler[8]. Based on these measurements, we will discuss the following points in the present work.

1. The applicability of the time–temperature superposition principle and the effect of the polar stickers on the terminal relaxation zone.
2. The analysis of the α^*_{DMA} relaxation with respect to its dependence on the degree of functionalization and temperature.
3. The comparison of the α^*_{DMA} relaxation analysis with recent dielectric measurements[11]. In these measurements, a second relaxation (α^*_{DS}) was observed at frequencies lower than the α relaxation, which is related to the dynamic glass transition. The temperature dependences of both the α and α^*_{DS} relaxations were described by the Williams–Landel–Ferry (WLF) equation[13]. Based on an analysis of the dielectric relaxation, the α^*_{DS} relaxation was associated with the complexation dynamics of binary contacts as predicted by the sticky reptation model. It will be of special interest to address the issue of how well both methods describe the same relaxation process.

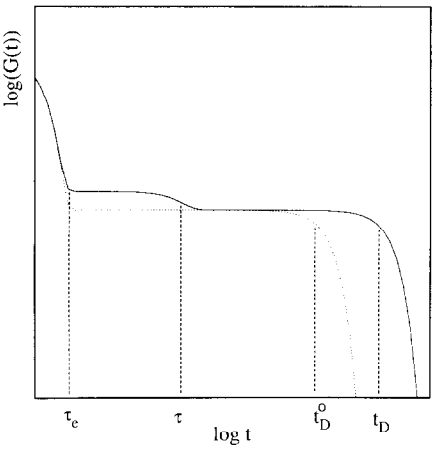

Figure 2 Stress relaxation modulus $G(t)$ of an entanglement network (· · · · ·) and a corresponding thermoreversible network with binary stickers (——) according to the LRC model, where τ_e represents the Rouse relaxation time of an entanglement strand, τ is the lifetime of reversibly crosslinked contacts and t_D and t_D^0 are the terminal relaxation times of thermoreversible and entanglement networks, respectively

EXPERIMENTAL

Sample preparation

Polybutadiene with a molecular weight M_n of 28 000 g mol^{-1} ($M_w/M_n = 1.05$) was prepared by anionic polymerization in cyclohexane. We used the same material as used in previous rheooptical experiments[10]. The synthesis of 4-phenyl-1,2,4-triazolidine-3,5-dione (phenylurazole) and the subsequent functionalization of the polybutadiene with various amounts of phenylurazole were carried out according to literature descriptions[14]. *Table 1* summarizes the sample codes, degrees of functionalization, numbers of urazole stickers per chain and glass transitions.

Dynamic mechanical measurements and data treatment

Rheological measurements were carried out with a Rheometrics RDA2 in the oscillatory mode. To cover a broad temperature range, parallel plates with diameters of 8 mm and 25 mm were used. The amplitudes were chosen to give the strongest force signal within the linear

Table 1 Sample codes, degrees of functionalization, numbers of urazole units per chain and corresponding glass transition temperatures (determined by dielectric spectroscopy[11])

Sample code	Degree of functionalization (mol% per double bond)	Number of urazole stickers per chain	Glass transition temperature (K)
PB-28-PU-0	0	0	175
PB-28-PU-2	2	10	177.5
PB-28-PU-3	3	16	178.7
PB-28-PU-4	4	21	182.5

viscoelastic region. Measurements were performed in the frequency range 0.0079–79.5 Hz with six measurements per decade. The temperature was varied between 193 K and 293 K in steps of 5 K.

Figures 3a and *3b* show typical sets of data for the storage modulus G' and the loss modulus G'' as a function of frequency for selected temperatures. The isothermal data $G'(\omega, T)$ were reduced to the reference temperature T_0 according to

$$G'_{red}(\omega, T) = G'(\omega, T)(T_0/T) \quad (2)$$

neglecting the density change with temperature[13]. These reduced data were used in the construction of isothermal master curves. Owing to the fact that the materials are thermorheologically complex (see below), the 'apparent' master curves are based on shifting the storage modulus data. The master curves for G', G'', J' and η' using these shift factors are shown in *Figures 6*, *7*, *8* and *10*. All viscoelastic quantities were plotted as a function of frequency ν (reciprocal time) instead of the commonly used radial frequency ω (radians per second) in order to compare the viscoelastic data directly with the dielectric measurements. Details of the dielectric experiments are reported elsewhere[11]. From the loss modulus master curves, the relaxation time spectra were calculated (*Figure 11*). Spectrum calculation was carried out with the commercially available Rheometrics RHECALC software using non-linear regression with fixed relaxation times.

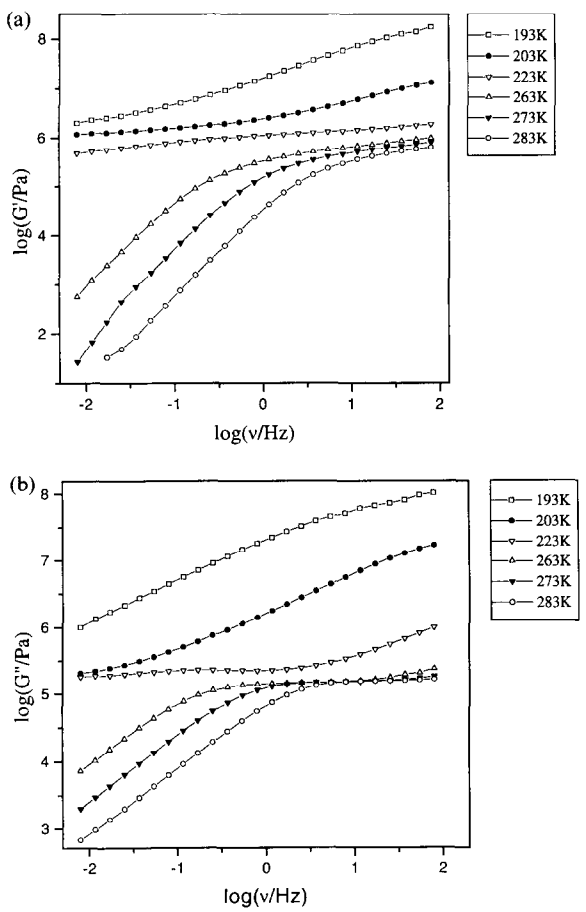

Figure 3 Isotherms of the storage modulus $G'(\nu)$ (a) and loss modulus $G''(\nu)$ (b) at various temperatures for a polybutadiene (M_n = 28 000 g mol^{-1}) modified by 4 mol% phenylurazole units

RESULTS

In *Figure 3a*, the storage modulus curves are shown as a function of frequency at different temperatures for a sample with 4 mol% polar stickers. The curves at high temperatures (263–283 K) correspond to the transition from the rubbery plateau (isotherm at 223 K) to the terminal flow and the curves at low temperatures (203 K, 193 K) show the upturn to the glass. In *Figure 3b*, the loss modulus curves of the same sample are shown for the same temperatures. Again the three relaxation regimes can be distinguished. The curve at 223 K shows a small dispersion maximum at a frequency (log ν) of about −0.7. This relaxation will be designated as the α^*_{DMA} relaxation in the following.

In *Figure 4*, this dispersion maximum (arrows) is shown at a temperature of 238 K for samples with different amounts of polar stickers. Obviously, the intensity of the signal corresponding to this relaxation process increases with the degree of functionalization (see later).

In *Figure 5*, the same relaxation process is shown as a function of temperature for a sample with 4 mol% polar stickers. In this representation the loss modulus curves are already reduced by multiplication with T_0/T (with T_0 = 233 K).

As described earlier, the apparent isothermal master curves of the storage modulus G' were obtained for a reference temperature of 233 K. In *Figure 6*, the G' master curves of samples with 0 mol%, 2 mol%, 3 mol%

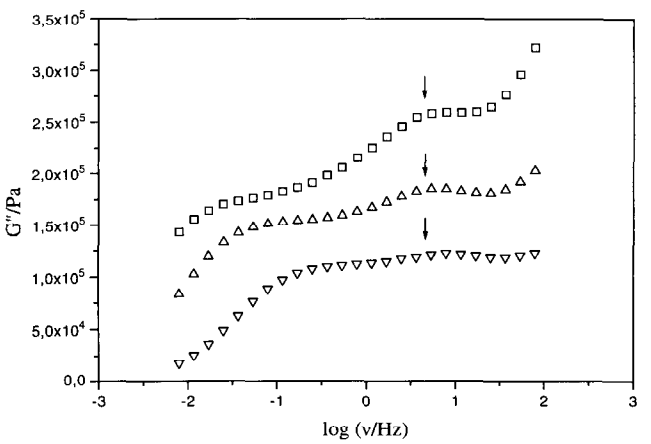

Figure 4 Loss modulus $G''(\nu)$ for polybutadiene PB-28-PU-X functionalized by 2 mol% (▽), 3 mol% (△) and 4 mol% (□) phenylurazole units (T = 238 K)

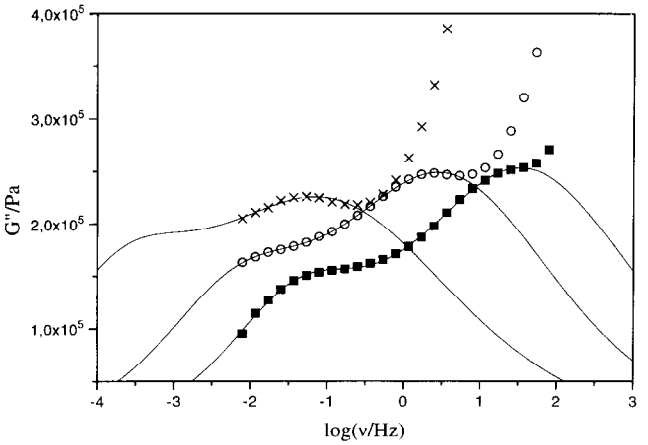

Figure 5 Loss modulus $G''(\nu)$ for polybutadiene PB-28-PU-4 at various temperatures in the rubber plateau regime: (■) 243 K; (○) 233 K; (X) 218 K. The solid lines represent the fitted curves according to the sum of two Havriliak–Negami functions (equation (6))

and 4 mol% polar stickers are compared. Applying the same shift factors to the G'' and η' curves leads to the master curves shown in *Figures 7* and *8*. In order to avoid overlap of the data, the G' and G'' master curves of the modified polybutadienes are vertically offset against each other by half a decade.

DISCUSSION

Applicability of the time–temperature superposition principle and the effect of the polar stickers on the terminal relaxation zone

As predicted by theory, three relaxation regimes can be distinguished. At low frequencies, a slope of nearly 2 (*Table 2*) in the log G' *versus* log νa_T curves reveals the transition to flow ('terminal relaxation'). At high frequencies, the transition to the glass can be observed. At intermediate frequencies between these two transitions, a rubbery plateau appears for all degrees of modification. The terminal relaxation is shifted to lower frequencies with increasing degree of functionalization.

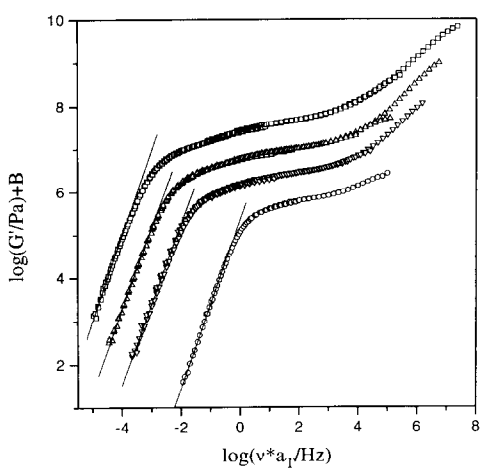

Figure 6 Storage modulus master curves $G'_{red}(\nu)$ (T_{ref} = 233 K) for PB-28-PU-X at different degrees of substitution: (○) 0 mol%; (▽) 2 mol%; (△) 3 mol%; (□) 4 mol%. The solid lines indicate the slope in the terminal zone. The master curves are vertically offset against each other by half a decade for clarity (logarithmic vertical shift B: PB-28-PU-0, 0; PB-28-PU-2, 0.5; PB-28-PU-3, 1; PB-28-PU-4, 1.5)

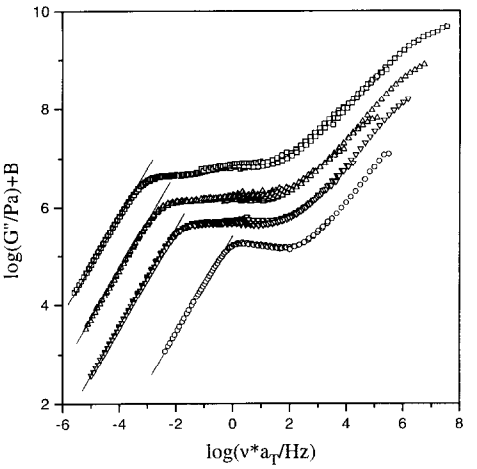

Figure 7 Loss modulus master curves $G''_{red}(\nu)$ (T_{ref} = 233 K) for PB-28-PU-X: (○) 0 mol%; (▽) 2 mol%; (△) 3 mol%; (□) 4 mol%. The master curves were obtained by using the shift factors a_T obtained from shifting the reduced storage modulus data. The solid lines indicate the behaviour in the terminal zone. The master curves are vertically offset for clarity (logarithmic vertical shift B: PB-28-PU-0, 0; PB-28-PU-2, 0.5; PB-28-PU-3, 1; PB-28-PU-4, 1.5)

As already mentioned earlier, the same shift factors were applied to all viscoelastic functions. The isothermal loss modulus master curves (*Figure 7*) are smooth in the terminal zone and in the glass transition regime. The slope in the terminal region is close or equal to 1 (*Figure 7*, straight lines; *Table 2*). In the rubbery plateau region the failure of TTS becomes obvious in the case of chains with stickers. As already outlined in the previous section, within the rubbery plateau region a small dispersion maximum is observed (*Figure 5*). Based on the prediction made by the sticky reptation theory[4], this maximum could be assigned to the local complex dynamics described by the equilibrium between closed (U_2) and free (U) stickers

$$U_2 \underset{k_+}{\overset{k_-}{\rightleftharpoons}} 2U \qquad (3)$$

With decreasing temperature this equilibrium is shifted to the left. This temperature dependence (see later)

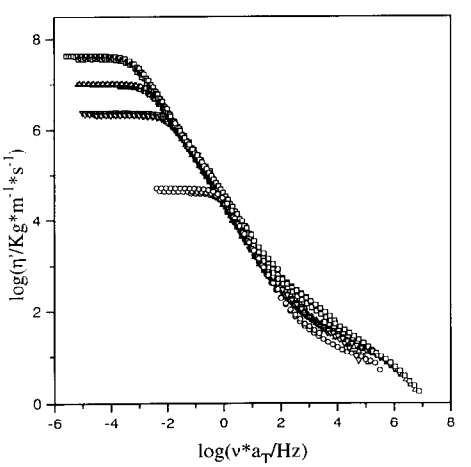

Figure 8 Master curves of the dynamic viscosity $\eta'_{red}(\nu)$ (T_{ref} = 233 K) for PB-28-PU-X: (○) 0 mol%; (▽) 2 mol%; (△) 3 mol%; (□) 4 mol%

Table 2 Slopes of the G' and G'' master curves in the terminal zone, zero shear viscosities, WLF parameters C_1, C_2 and products C_1C_2 obtained from dynamic mechanical analysis for polybutadienes with different amounts of polar stickers ($T_{ref} = 233$ K)

Sample code	G' terminal slope	G'' terminal slope	log η_0	C_1	C_2 (K)	C_1C_2 (K)
PB-28-PU-0	1.95	0.99	4.705	5.68	101.66	577.43
PB-28-PU-2	1.86	1.00	6.306	11.66	150.2	1751.38
PB-28-PU-3	1.89	0.99	6.990	11.85	136.84	1621.54
PB-28-PU-4	1.98	0.99	7.62	13.2	141.2	1864.2

makes time–temperature superposition impossible, and thus within the rubbery plateau region the functionalized samples exhibit thermorheologically complex behaviour.

If one considers the low frequency regime of the master curves for the dynamic viscosity (*Figure 8*), an increase in the zero shear viscosity with increasing degree of modification is observed. Furthermore, the turnover from non-Newtonian behaviour to Newtonian behaviour is shifted to lower frequencies with increasing degree of substitution. Both results have already been recognized in earlier work[12]. In *Figure 9* the increase in the zero shear viscosity is demonstrated. Data from earlier work are included and show good agreement with the present measurements. The zero shear viscosity is very sensitive to the molecular weight of the sample. Thus, the observed increase in viscosity could be interpreted as an apparent increase in the molecular weight caused by linking of the chains via hydrogen bonds.

Whereas the zero shear viscosity depends on the molecular weight and is not much affected by the molecular weight distribution, the real part of the creep compliance J' in the low shear rate limit (J_e^0) is very sensitive to the molecular weight distribution. In *Figure 10*, the log J' master curves are plotted against log G' as obtained from the isothermal master curves at 233 K. For monodisperse polymers above the entanglement molecular weight, reptation theory predicts that J_e^0 will be independent of the molecular weight[13]. In the case of the unsubstituted polybutadiene, a constant value of J_e^0 at about $10^{-5.5}$ N m^{-2} is obtained. This is consistent with earlier work[12]. The introduction of polar groups leads to an increase in the steady-state compliance. Thus, the polar stickers cause a broadening of the molecular weight distribution. The relaxation time spectra (*Figure 11*) lead to the same conclusion. The relaxation time distribution increases with increasing degree of modification. This difference is most pronounced between the samples with 2 mol% and 3 mol% polar stickers. The increase in the steady-state compliance and the broadening of the relaxation time distribution are less pronounced than in earlier measurements[12]. This is probably because of the lower polydispersity of the starting polybutadiene used for the present samples. Recent stress-optical experiments with the same materials also show a broadening of the relaxation time distribution[10].

Despite the fact that TTS fails, we attempted an analysis of the shift factors obtained from shifting the G' data. Using the linearized form of the WLF equation[13], the parameters C_1 and C_2 were obtained for a reference temperature of 233 K. *Table 2* summarizes these parameters and the products C_1C_2. Two important features are observed: first, the WLF parameters are much higher than expected for conventional linear polymers; secondly, both parameters, and consequently the product C_1C_2, increase with the number of polar units. This would correspond to an increased apparent flow activation energy. These results are basically identical to those reported earlier[12].

Analysis of the α^*_{DMA} relaxation

In the case of the functionalized samples, a small step in the log G' curves occurs within the rubbery plateau region. On the basis of the LRC model, this relaxation process (the α^*_{DMA} relaxation) can be interpreted in terms of the process related to the dynamics between uncomplexed and complexed stickers. At frequencies higher than this relaxation process, the polar stickers act

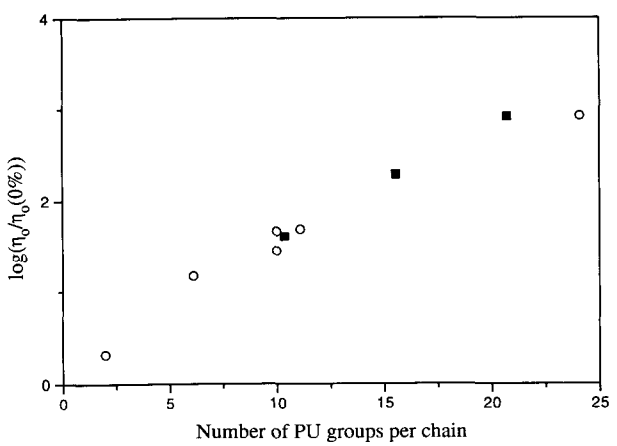

Figure 9 Enhancement of the zero shear viscosity as a function of the number of phenylurazole groups per chain. In addition to the experimental data from the present work (■), earlier data[12] are included (○) which come from samples with different molecular weights and degrees of substitution

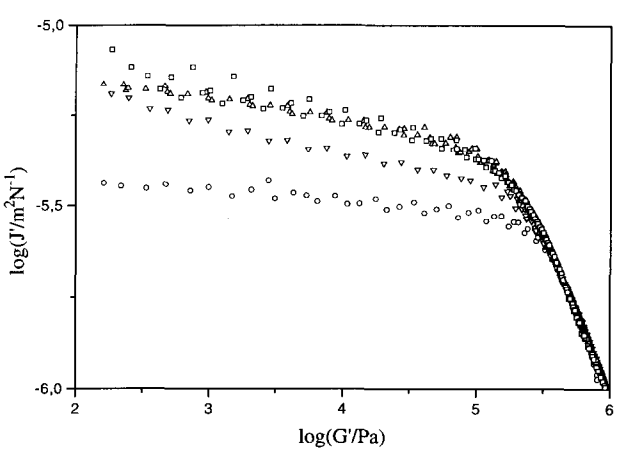

Figure 10 Real part of the complex creep compliance J'_{red} (ν) as a function of the storage modulus G'_{red} (ν) for PB-28-PU-X: (○) 0 mol%; (▽) 2 mol%; (△) 3 mol%; (□) 4 mol%

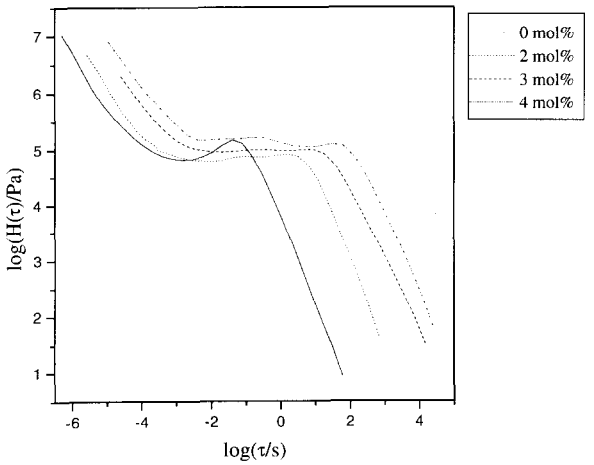

Figure 11 Relaxation time spectra for polybutadienes with different degrees of substitution, as calculated from the loss modulus master curve

like covalent crosslinks (pseudocovalent network), whereas at lower frequencies the system behaves like an entanglement network (pseudoentanglement network). Thus, we can define two rubbery plateaus: one at which the junction dynamics are slow ($G_N^0(U_2)$), i.e. $\nu_{exp} > \nu(\alpha^*_{DMA})$, and one at which the junction dynamics are fast ($G_N^0(U)$), i.e. $\nu_{exp} < \nu(\alpha^*_{DMA})$. The values of $G_N^0(U_2)$ and $G_N^0(U)$ are taken as the storage modulus values $G'(\nu)$ at the frequencies where tan δ has its minima in the plateau zone. According to this method[15] and our previous experience[16], this type of analysis allows the determination of the plateau modulus to within ±5%. Though this way of determination of the plateau modulus has some uncertainty, the data show that the plateau modulus $G_N^0(U_2)$ increases with increasing degree of functionalization according to an increased number of pseudocovalent crosslinks, whereas $G_N^0(U)$ appears to be independent of the number of polar stickers, as is expected for a pseudoentanglement network (*Table 3*). The plateau moduli $G_N^0(U)$ of the modified samples are slightly lower than the plateau modulus of unmodified polybutadiene. This is because for the unmodified polybutadiene, $G_N^0(U)$ is taken at a frequency slightly below the glass transition, whereas the plateau moduli $G_N^0(U)$ of the modified samples are taken near the terminal relaxation. In earlier measurements[12], the distinction between $G_N^0(U_2)$ and $G_N^0(U)$ was not made. The values obtained for the plateau moduli are between those values of $G_N^0(U_2)$ and $G_N^0(U)$ reported here.

The difference between the two moduli $G_N^0(U_2)$ and $G_N^0(U)$ increases with increasing degree of modification. From this difference it should be possible to calculate the number of reversible contacts n_{plat} per unit volume according to the equation

$$n_{plat}kT = G_N^0(U_2) - G_N^0(U) = \Delta G \quad (4)$$

where k is the Boltzmann constant and $T = 233$ K. The results are given in *Table 3*. In principle, the same calculation should be possible with the relaxation strength ΔG that is obtained from a Havriliak–Negami fit of the $G''(\nu)$ isotherms (*Figure 4*). Since two other relaxation processes interfere, the terminal relaxation and the dynamic glass transition, the error in the determination of the relaxation strength is too large to allow its use for such a calculation.

From the molecular weight M_n, the density ρ and the number of stickers per chain x (*Table 1*), it is possible to calculate a theoretical number of crosslinks n_{theo} under the condition that all stickers are closed

$$n_{theo} = (\rho/M_n)N_A x \quad (5)$$

where N_A is the Avogadro constant.

The number of crosslinks that results from the theoretical calculation is larger than that obtained from the plateau modulus difference. This implies that not all contacts are closed. From the relation between n_{plat} and n_{theo}, the fraction of closed stickers can be calculated (*Table 3*). According to this calculation, about 60–70% of the stickers are complexed. The values are close to the fraction of closed stickers p obtained by i.r. measurements[9].

In order to obtain information about the temperature dependence of the α^* process which appears within the rubbery plateau region, those isotherms for which this process could be identified unambiguously were examined. *Figure 5* shows this relaxation process for a degree of functionalization of 4 mol% phenylurazole at three temperatures.

The data at 243 K (filled squares) and at 233 K (open circles) show three relaxation regimes for the polymer. At low frequencies, a weakly developed maximum reveals the transition from the rubbery plateau to the flow region. At higher frequencies, a second maximum appears which, according to the hindered reptation theory, corresponds to the breaking of dimeric contacts. At even higher frequencies, a strong increase in the out-of-phase modulus G'' reveals the onset of the glass transition.

Neglecting the upturn to the glass at high frequencies, the isotherms can be described by means of the sum of two Havriliak–Negami functions[17] which are also useful in describing the dielectric relaxation

$$G^*(\omega) = \frac{\Delta G}{[1 + (i\omega\tau)^\alpha]^\beta} \quad (6)$$

Table 3 Plateau moduli and numbers of U_2 crosslinks for PB-28-PU-X ($T_{ref} = 233$ K). The moduli refer to the relaxation regimes of the rubbery plateau region where the systems behave like pseudocovalent networks ($G_N^0(U_2)$) and as pseudoentanglement networks ($G_N^0(U)$). The value of n_{plat} is calculated from the plateau modulus difference and n_{theo} is the number of reversible crosslinks if the fraction of closed stickers is unity

Sample code	Plateau modulus 10^{-5} $G_N^0(U_2)$ (Pa)	Plateau modulus 10^{-5} $G_N^0(U)$ (Pa)	10^{-5} $[G_N^0(U_2) - G_N^0(U)]$ (Pa)	n_{plat} (mol^{-1} l)	n_{theo} (mol^{-1} l)	$p = n_{plat}/n_{theo}$
PB-28-PU-0		6.1			0	
PB-28-PU-2	8.7	3.9	4.8	0.25	0.32	0.77
PB-28-PU-3	9.6	3.6	6	0.31	0.51	0.61
PB-28-PU-4	13.6	4	9.6	0.50	0.67	0.74

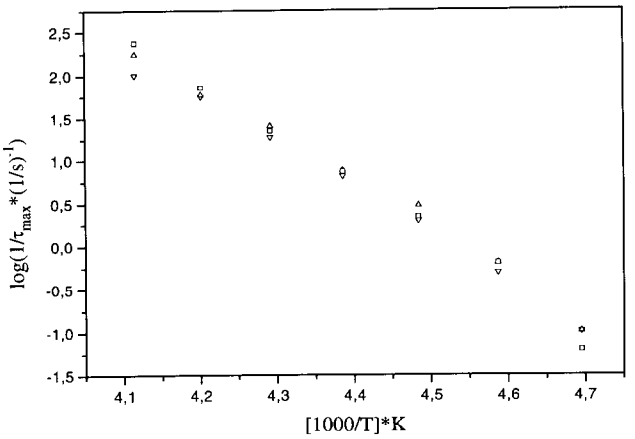

Figure 12 Temperature dependence of the α^*_{DMA} relaxation (measured by dynamic mechanical measurements) for PB-28-PU-*X*: (▽) 2 mol%; (△) 3 mol%; (□) 4 mol%

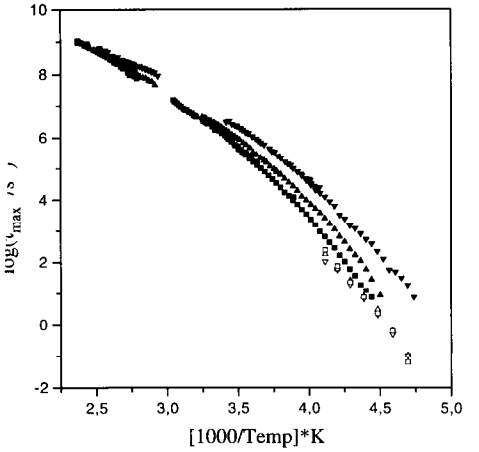

Figure 13 Temperature dependence of the α^* relaxation measured by dielectric (τ^*_{DS}) and dynamic mechanical (τ^*_{DMA}) measurements for PB-28-PU-*X* (open symbols, dynamic mechanical measurements; filled symbols, dielectric measurements): (▽) 2 mol%; (△) 3 mol%; (□) 4 mol%

To apply this function to dynamic mechanical data, the complex dielectric function $\varepsilon^*(\omega)$ has to be substituted by the complex shear modulus $G^*(\omega)$. ΔG corresponds to the area under the G'' curve. The parameters α and β describe the symmetric and asymmetric broadening of the relaxation time distribution. In the subsequent fits, no asymmetric broadening was considered, i.e. β was fixed at unity.

At temperatures for which the terminal zone lay outside the experimental frequency range (i.e. data at 218 K; crosses in *Figure 5*), the maximum frequency ν and thus the relaxation time τ of the terminal relaxation were estimated via the shift parameter a_T according to

$$\nu = \frac{\nu_{ref}}{a_T} \tag{7}$$

where ν_{ref} is the maximum frequency at the reference temperature T_{ref}. The parameters α and ΔG of the terminal relaxation were taken from the fit, where the terminal relaxation was completely located in the experimental frequency range. By this method, data in the temperature range 213–243 K were fitted. Though the determination of the parameters α and ΔG is not very exact, the relaxation time τ can be determined quite accurately.

From the fits, the relaxation time of the α^*_{DMA} relaxation within the rubbery plateau was obtained for different temperatures. In *Figure 12*, the temperature dependences of the relaxation times for three different degrees of modification are shown.

According to the sticky reptation model[4], the average lifetime τ of the stickers ($= \tau(\alpha^*_{DMA}$ relaxation)) is correlated to the terminal relaxation time t_D via

$$\tau = t_D \frac{(N_e/N)[1 - (9/p) + (12/p^2)]}{2S^2} \tag{8}$$

where N is the number of monomers per chain, N_e is the number of monomers per entanglement (*Table 4*) (calculated from G^0_N(U), *Table 3*), S is the number of stickers per chain, p is the fraction of closed stickers (*Table 3*) and t_D is the terminal relaxation time as obtained from the Havriliak–Negami fits.

In *Table 4*, the relaxation times $\tau_{theo}(\alpha^*_{DMA}$ relaxation) as calculated from equation (8) are compared to the corresponding relaxation times $\tau_{HN}(\alpha^*_{DMA}$ relaxation) obtained from the Havriliak–Negami fits. For the PB-28-PU-4 sample where the plateau modulus difference and thus N_e can be calculated with the highest accuracy, the correlation between the terminal relaxation time and the average lifetime of the stickers appears to be described perfectly well by the sticky reptation theory.

Assuming Arrhenius-type behaviour, the activation energy of the α^*_{DMA} relaxation is obtained from the slope of a plot such as those shown in *Figure 12*. Though at first sight all samples seem to result in the same activation energy, a linear regression gives slightly different values for the individual samples as shown in *Table 4*.

Both the extremely high activation energy and the large frequency factor A indicate that the α^*_{DMA} relaxation cannot be ascribed to a truly local process. As proposed by the sticky reptation model, the rupture/formation of a binary contact is combined with a

Table 4 Relaxation times τ_{HN} (α^*_{DMA} relaxation) as obtained from the Havriliak–Negami fits compared to τ_{theo} (α^*_{DMA} relaxation) as obtained from the sticky reptation theory. The values of the terminal relaxation times t_D and the numbers N_e of monomers per entanglement without stickers that were needed for the theoretical calculations are also shown

Sample code	t_D (s)	N_e	$\tau_{HN}(\alpha^*_{DMA}$ relaxation) (s)	τ_{theo} (α^*_{DMA} relaxation) (s)
PB-28-PU-2	2.53	83	0.04	0.02
PB-28-PU-3	11.0	90	0.04	0.07
PB-28-PU-4	24.5	81	0.05	0.05

Table 5 Activation energies and frequency factors A calculated according to the Arrhenius equation $\log(1/\tau) = A - (E_a/2.3RT)$ from dielectric spectroscopy and dynamic mechanical measurements. The analysis was restricted to the temperature interval where the analysis of the α^* relaxation could be performed in the dynamic mechanical experiment

Sample code	E_a [a] (kJ mol^{-1})	Logarithmic frequency factor A^a	E_a [b] (kJ mol^{-1})	Logarithmic frequency factor A^b
PB-28-PU-2	98.8	23.2	101.5	26.1
PB-28-PU-3	103.5	24.5	106.3	26.3
PB-28-PU-4	112.5	26.6	113.9	27.3

[a] From dynamic mechanical analysis
[b] From dielectric spectroscopy

diffusion of those chain segments adjacent to the sticker. The cooperative character of this chain diffusion is reflected in the high activation energy and the large apparent frequency factor.

Comparison with dielectric measurements

In *Figure 13*, the temperature dependence of the relaxation times obtained in dynamic mechanical measurements is compared to the dielectric data for the α^*_{DS} relaxation, which corresponds to the complexation dynamics of dimeric complexes.

While for the PB-28-PU-4 sample both data sets show rather good agreement, the difference between the relaxation times obtained by dynamic mechanical measurements and dielectric measurements is about 0.8 decades in the case of PB-28-PU-3 and 1.6 decades for PB-28-PU-2. The process observed by dynamic mechanical measurements (α^*_{DMA}) appears at lower frequencies than the corresponding dielectric process (α^*_{DS}). While the dielectric data decrease in magnitude with increasing degree of modification, the relaxation times obtained by dynamic mechanical spectroscopy do not depend significantly on the number of stickers. As was outlined in previous work[11], the increase in the dielectric relaxation times with increasing degree of modification is mainly due to an increase in the glass transition temperature. Obviously, the process corresponding to the dielectric relaxation is coupled in some way to the dynamic glass transition of polybutadiene, whereas in dynamic mechanical measurements this coupling is not observed. Further studies are necessary for a deeper understanding of these phenomena[18].

The temperature dependences of the relaxation times obtained by both methods are in rather good agreement. Taking those dielectric data which are in the temperature range covered by dynamic mechanical measurements, a linear regression leads to activation enthalpies and frequency factors which are in good agreement with the values obtained by dynamic mechanical measurements (*Table 5*).

Both methods show an increase in the activation enthalpy with increasing degree of functionalization. An analysis of the dielectric data over the whole temperature range leads to the same result[11]. This can be interpreted on the basis of a theoretical description given by Nyrkova *et al.*[19]. This theory deals with the formation of dipole–dipole clusters in ionomers, showing that the stability of multiplets is enhanced in comparison to isolated dimeric clusters. With increasing degree of substitution, the probability increases that two dimeric complexes are close neighbours. As a consequence, double or triple clusters of dimers or, in general, multiplets with a correspondingly higher stability are formed.

ACKNOWLEDGEMENTS

This work was supported by the Fonds der Chemischen Industrie through stipends for U. Seidel and M. Müller. M. Müller is indebted to C. Böffel and H. W. Spiess for their support. R. Stadler acknowledges further support from 'Deutsche Kautschukgesellschaft DKG' and the Deutsche Forschungsgemeinschaft (SFB262). The authors are indebted to Liane Freitas, R. Colby, G. Fuller and L. Leibler for numerous discussions concerning this work.

REFERENCES

1 Burchard, W. and Ross-Murphy, S. B. (Eds) 'Physical Networks', Elsevier Applied Science, London, 1988
2 Gonzales, A. E. *Polymer* 1983, **24**, 77
3 Gonzales, A. E. *Polymer* 1984, **25**, 1469
4 Leibler, L., Rubinstein, M. and Colby, R. H. *Macromolecules* 1991, **24**, 4701
5 Stadler, R. and de Lucca Freitas, L. *Colloid Polym. Sci.* 1986, **264**, 773
6 Stadler, R. *Prog. Colloid Polym. Sci.* 1987, **75**, 140
7 de Lucca Freitas, L. and Stadler, R. *Colloid Polym. Sci.* 1988, **266**, 1095
8 Colby, R. H. and Stadler, R. unpublished results
9 de Lucca Freitas, L., Auschra, C., Abetz, V. and Stadler, R. *Colloid Polym. Sci.* 1991, **269**, 566
10 Seidel, U., Stadler, R. and Fuller, G. G. *Macromolecules* 1994, **27**, 2066
11 Müller, M., Kremer, F., Stadler, R., Fischer, E. W. and Seidel, U. *Colloid Polym. Sci.* 1995, **273**, 38
12 de Lucca Freitas, L. and Stadler, R. *Macromolecules* 1987, **20**, 2478
13 Ferry, J. D. 'Viscoelastic Properties of Polymers', 3rd Edn, Wiley, New York, 1980
14 Stickler, J. C. and Pirkle, W. H. *J. Org. Chem.* 1966, **31**, 3444
15 Wu, S. *J. Polym. Sci., Polym. Phys. Edn* 1987, **25**, 557
16 de Araujo, M. A. and Stadler, R. *Makromol. Chem.* 1988, **189**, 2169
17 Havriliak, S. and Negami, S. *Polymer* 1967, **8**, 161
18 Müller, M., Stadler, R., Kremer, F. and Williams, G. *Macromolecules* (submitted)
19 Nyrkova, I. A., Khokhlov, A. R. and Doi, M. *Macromolecules* 1993, **26**, 3601